We are IntechOpen,
the world's leading publisher of
Open Access books
Built by scientists, for scientists

6,900
Open access books available

185,000
International authors and editors

200M
Downloads

154
Countries delivered to

Our authors are among the

TOP 1%
most cited scientists

12.2%
Contributors from top 500 universities

Interested in publishing with us?
Contact book.department@intechopen.com

Multiscale Window Interaction and Localized Nonlinear Hydrodynamic Stability Analysis

X. San Liang*

1Harvard University, School of Engineering and Applied Sciences, Cambridge, MA
2Central University of Finance and Economics, Beijing
3Stanford University, Center for Turbulence Research, Stanford, CA
4Nanjing Institute of Meteorology, Nanjing
1,3USA
2,4China

1. Introduction

Hydrodynamic stability has been a subject extensively investigated in fluid dynamics (see Lin 1966, Drazin & Reid 1982; Godreche & Manneville 1998; Schmid & Henningson 2001, and references therein). We still lack, however, a stability analysis capable of operationally handling results from experiments and numerical simulations, or data taken directly from nature. These "real problems", as we will hereafter refer to, are in general highly nonlinear and localized in space and time. In other words, the signal tends to be temporally intermittent, the regions of interest may be finitely and irregularly defined, and the definition domain could be on the move. Specific examples include atmospheric cyclogenesis, ocean eddy shedding, vortex shedding behind bluff bodies, emergence of turbulent spots, among many others. In this study, we present a new approach to address this old issue, and show subsequently how this approach can be conveniently used for the investigation of a variety of fluid flow problems which would otherwise be very difficult, if not impossible, to investigate.

Localization and admissibility of finite amplitude perturbation are the two basic requirements for the approach. Classically, stability in terms of normal modes (e.g., Drazin & Reid 1982) organizes the whole domain together to make one dynamical system; stability defined in the sense of Lyapunov is measured by a norm (energy) of the perturbation over the whole spatial domain (cf. section 2). These definitions do not retain local features. On the other hand, many analyses have been formulated aiming at localized features, among which the geometrical optics stability method (Lifschitz 1994) and the Green function approach for convective/absolute instability study (Briggs 1964; Huerre & Monkewitz 1990; Pierrehumbert & Swanson 1995) now become standard. These approaches, though localized, usually rely on small perturbation approximation to make linearization possible.

We integrate the philosophies of the above two schools to build our own methodology, which retains full physics, and admits arbitrary perturbation, particularly perturbation of local dynamics, finite amplitude and variable spatial scales. The basic idea is that: The Lyapunov type norm (energy) could be "localized" to make a spatio-temporal field-like metric. In doing

---

*URL:http://people.seas.harvard.edu/~san

so the stability of a system gains a "structure" (which is a more reasonable representation of nature), and the system is organized into structures of distinct processes. The approach is Eulerian. It does not rely on trajectory calculation for local dynamics.

The problem now becomes how to achieve the Lyapunov norm localization. In the next section, we show how a hydrodynamic stability is defined in the Lyapunov sense, and what the definition really implies. We then show that it could be connected to our previous work on mean-eddy interaction within classical framework (section 3), provided that a suitable multiscale decomposition is used. The decomposition is fulfilled with a new mathematical machinery called *multiscale window transform*, (section 4), on the basis of which our instability analysis is formulated. Sections 5-8 are devoted to the establishment of the formalism. Toward the end of this study, we present two real problem applications. The first is a dynamical interpretation of a rather complicated oceanic circulation which has been a continuing challenge since 70 years ago (section 9); we will see in there that the problem becomes straightforward within our framework. The other one is about the vortex shedding, turbulence production, laminarization, and structure sustaining in a turbulent wake behind a circular cylinder (section 10). This study is summarized in section 11.

2. Lyapunov stability

A fundamental definition of hydrodynamic stability was introduced by Lyapunov (cf. Godreche and Manneville, 1998). Given a flow, let $\xi = \xi(\mathbf{x}, t)$ stand for a snapshot of its state, and $\Xi = \Xi(\mathbf{x}, t)$ for a basic solution, which could be a fixed point or any time-varying equilibrium (limiting cycle, for example). In the sense of Lyapunov, the stability of Ξ can be defined as follows: For any $\varepsilon > 0$, if there is a $\delta = \delta(\varepsilon) > 0$, such that

$$\|\xi(\mathbf{x}, t_1) - \Xi(\mathbf{x}, t_1)\| < \varepsilon, \tag{1}$$

$$\text{as} \quad \|\xi(\mathbf{x}, t_0) - \Xi(\mathbf{x}, t_0)\| < \delta, \tag{2}$$

for all $t_1 > t_0$, then Ξ is stable; otherwise it is unstable. Here the norm is defined to be such that $\|\xi\| = \left[\int_\Omega \xi^T \xi d\mathbf{x}\right]^{1/2}$ for ξ over the whole domain Ω, where the superscript T stands for a transpose when ξ is a vector.

Observe that, given a time interval Δ, the basic solution Ξ may be approximately understood as a reconstruction of ξ in time on some slow manifold. In this sense, the terms in the norms of (1) and (2) are actually the perturbations from the slow reconstruction at time instants t_1 and t_0, respectively. Note the norm in the definition can be essentially replaced by its square, so the left hand sides are related to the perturbation energy growth on this interval, recalling how the Parseval relation connects $\int_\Delta (\xi - \Xi)^T (\xi - \Xi) \, dt$ to the perturbation energy. (Note $(\xi - \Xi)^T (\xi - \Xi)$ itself is not the perturbation energy.)

Another observation is about the spatial integration of the norm, which is taken over the whole domain Ω for a closed system. It is this very integration that eliminates the local features and accordingly makes the Lyapunov stability analysis inappropriate for localized events. We need to see what it really means.

It has been observed in real fluid problems, particularly in atmosphere-ocean problems (e.g., Gill 1982), that a fluid system, though complex, often displays a combination of two independent components: a transport and a transfer. The transport component reveals itself in a form like advection and propagation, while the transfer results in the local growth of disturbances. One may intuitively argue that these two processes are both a kind of energy

redistribution process. The former redistributes energy in physical space, while the latter redistributes energy between the basic state and the perturbed state. This implies that a transport should integrate to zero over a closed domain; in other words, it has a divergence form in mathematical expression. The integration in the Lyapunov definition serves to eliminate any transport process that may exist, resulting in a pure transfer component over the domain. Therefore, underlying the Lyapunov definition is essentially about the transfer from the basic state to the perturbation. This makes sense, as physically an instability is actually a process of energy transfer between the two states.

Therefore, the problem of hydrodynamic stability is fundamentally a problem about the interaction between the basic state and the perturbation, which is measured by the energy transfer between them. The above physical clarification implies that we may localize the Lyapunov norm if we can separate the transfer from the transport. In that case, there is no need to take the integration, and hence the transfer thus obtained is a spatio-temporal field. All the problem is now reduced to how to achieve the separation.

3. Mean-eddy interaction within the Reynolds decomposition framework

Liang (2007) achieved the separation within the framework of Reynolds decomposition. Originally his formalism was developed in the statistical context, i.e., a Reynolds average is understood as an ensemble mean or mathematical expectation with probability measure. The idea can be best elucidated with the evolution of a passive scalar advected by an incompressible flow $\mathbf{v}$:

$$\frac{\partial T}{\partial t} + \nabla \cdot (\mathbf{v}T) = 0. \tag{3}$$

Decompose T into a mean part and an eddy part:: $T = \bar{T} + T'$. It is easy to obtain the equations governing the mean energy and eddy energy (variance) (e.g., Lesieur, 1990)

$$\frac{\partial \bar{T}^2/2}{\partial t} + \nabla \cdot (\bar{\mathbf{v}}\bar{T}^2/2) = -\bar{T}\nabla \cdot (\overline{\mathbf{v}'T'}) \tag{4}$$

$$\frac{\partial \overline{T'^2/2}}{\partial t} + \nabla \cdot (\overline{\mathbf{v}T'^2/2}) = -\overline{\mathbf{v}'T'} \cdot \nabla \bar{T}. \tag{5}$$

It has been a tradition to classify the energetics so that terms in a divergence form stand out, just like what is done here. The divergence terms are conventionally understood as the transports of the mean and eddy energies, while the other terms singled out from the nonlinear processes are the "transfers". However, as pointed out by Liang (2007), the right hand sides of (4) and (5) do not cancel out—in fact, they sum to $\nabla \cdot (\bar{T}\overline{\mathbf{v}'T'})$, which is in general not zero.[1] As a result, they cannot represent the transfer process, which is by physics a redistribution of energy between the decomposed subspaces.

In his study, Liang (2007) established a rigorous formalism for the transfer. By his result, corresponding to (4) and (5) are the following two equations:

$$\frac{\partial \bar{T}^2/2}{\partial t} + \nabla \cdot \mathbf{Q}_0 = -\Gamma, \tag{6}$$

---

[1] A term $\nabla \cdot \overline{\mathbf{v}'T'}\bar{T}$ may be added to both sides of Eq. 4 to ensure that cancellation (see, for example, Pope, 2003). But physically it is not clear where this extra term comes from, and why it should be there.

$$\frac{\partial \overline{T'^2/2}}{\partial t} + \nabla \cdot \mathbf{Q}_1 = \Gamma, \tag{7}$$

where

$$\mathbf{Q}_0 = \frac{1}{2}\left[\bar{\mathbf{v}}\bar{T}^2 + \bar{T}\overline{\mathbf{v}'T'} \right], \qquad \mathbf{Q}_1 = \frac{1}{2}\left[\overline{\mathbf{v}T'^2} + \bar{T}\overline{\mathbf{v}'T'} \right], \tag{8}$$

$$\Gamma = \frac{1}{2}\left[\bar{T}\nabla \cdot (\overline{\mathbf{v}'T'}) - (\overline{\mathbf{v}'T'}) \cdot \nabla \bar{T} \right]. \tag{9}$$

This way the energy processes are separated into a transport, which is in a divergence form, and a transfer Γ, which sums to zero over the decomposed subspaces. The separation is unique. Because of the "zero-sum" property, and its similarity in form to the Poisson bracket in Hamiltonian mechanics, Γ has been called *canonical transfer*,[2] in distinction from other transfers one may have encountered in the literature.

A hydrodynamic stability analysis is thus fundamentally a problem of finding the canonical transfer. But the above Γ still cannot make the metric of hydrodynamic stability. As we argued before, a hydrodynamic stability in the Lyapunov sense is defined with respect to a decomposition in time. Within the Reynolds decomposition framework, this was fulfilled with a time averaging, as Liang (2007) discussed. But the time averaging applies only when a system is stationary, while unstable processes are in nature not stationary at all. Besides, if a decomposition is achieved through a time averaging, the eddy energy [e.g., the $\frac{1}{2}\overline{T'^2}$ in (7)] does not have time dependence. As a result, there would be no eddy energy growth in the Lyapunov definition. We need to generalize the traditional mean-eddy decomposition to resolve these issues.

4. Scale window and multiscale window transform

The *multiscale window transform* developed by Liang and Anderson (2007) is such a generalization. It extends the traditional mean-eddy decomposition to retain local physics, and to allow for interactions beyond the mean and eddy processes, e.g., the mean-eddy-turbulence interaction. This section gives it a brief introduction.

4.1 Scale window and multiscale window transform

An MWT organizes a signal into several distinct time scale ranges, while retaining its track in physical space. These time scale ranges form mutually exclusive *scale windows* which we hereafter define. The definition could be over a univariate interval, or a multi-dimensional domain; in the context of this study, it is univariate as we only deal with time. Consider a Hilbert space $V_{\varrho,j} \subset L_2[0,1]$. It is generated by $\{\phi_n^j(t)\}_{n=0,1,...,2^{j\varrho}-1}$, where

$$\phi_n^j(t) = \sum_{\ell=-\infty}^{+\infty} 2^{j/2}\phi[2^j(t+\varrho\ell) - n + 1/2]$$

(n runs through $\{0, 1, ..., 2^{j\varrho-1}\}$, $\phi(t)$ is a scaling function constructed via orthonormalization from cubic splines (Fig. 1, see Strang and Nguyen 1997), and $\varrho = 1$ and $\varrho = 2$ corresponding to the periodic and symmetric extension schemes, respectively. The periodic extension and symmetric extension are two commonly used schemes (see Liang and Anderson, 2007). In the spanning basis the scheme dependence is suppressed for notational simplicity, but one should be aware of the fact that different extension schemes may give different results. For

---

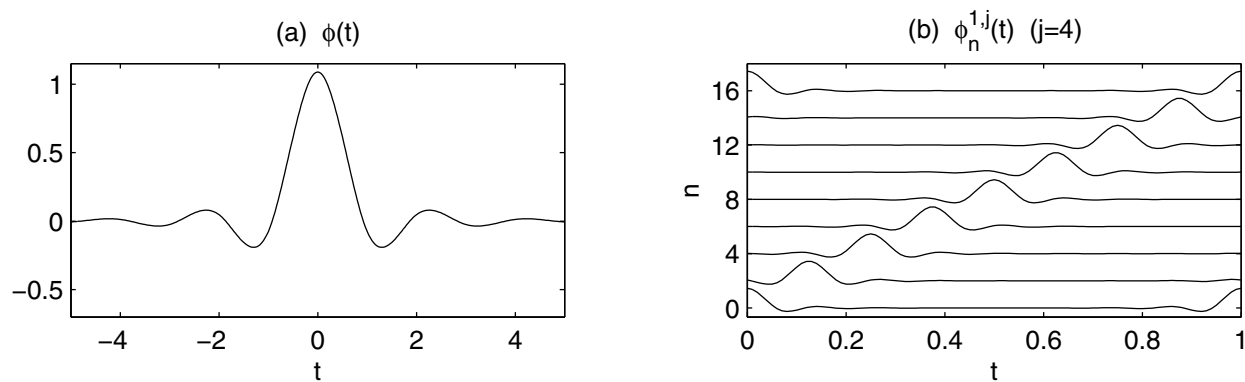[2] Originally it was termed "perfect transfer" in Liang (2007).

Fig. 1. (a) Scaling function ϕ constructed via cubic spline orthonormalization (Liang and Anderson, 2007). (b) Basis periodized from ϕ.

any integers $j_0 < j_1 < j_2$, it has been shown that the inclusion $V_{\varrho,j_0} \subset V_{\varrho,j_1} \subset V_{\varrho,j_2}$ holds (see Liang and Anderson, 2007). Thus a decomposition can be made such that

$$
\begin{aligned}
V_{\varrho,j_2} &= V_{\varrho,j_1} \oplus W_{\varrho,j_1-j_2} \\
&= V_{\varrho,j_0} \oplus W_{\varrho,j_0-j_1} \oplus W_{\varrho,j_1-j_2}
\end{aligned}
\tag{10}
$$

where W_{ϱ,j_1-j_2} is the orthogonal complement of V_{ϱ,j_1} in V_{ϱ,j_2}, and W_{ϱ,j_0-j_1} the orthogonal complement of V_{ϱ,j_0} in V_{ϱ,j_1}. It has been shown that V_{ϱ,j_0} contains scales larger than 2^{-j_0} only, while in W_{ϱ,j_0-j_1} and W_{ϱ,j_1-j_2} live the scale ranges between 2^{-j_0} to 2^{-j_1} and 2^{-j_1} to 2^{-j_2}, respectively (Liang and Anderson, 2007). These three subspaces of V_{ϱ,j_2} are referred to as, respectively, large-scale window (or mean window), meso-scale window (or eddy window), and sub-mesoscale window (or turbulence window). More windows can be likewise defined, but in this context, three are enough; in fact only two are concerned in most cases.

Suppose $p(t)$ is a realization of some function in $L_2[0,1]$, Liang and Anderson (2007) justified that p always lies in V_{ϱ,j_2} for some j_2 large enough. With the above basis, there is a scaling transform:

$$
\widehat{p}_n^j = \int_0^\varrho p(t)\phi_n^j(t)\, dt,
\tag{11}
$$

for any scale level j. Given window bounds $j_0 < j_1 < j_2$, p then can be reconstructed on the three windows formed above:

$$
p^{\sim 0}(t) = \sum_{n=0}^{2^{j_0}\varrho-1} \widehat{p}_n^{j_0}\phi_n^{j_0}(t),
\tag{12}
$$

$$
p^{\sim 1}(t) = \sum_{n=0}^{2^{j_1}\varrho-1} \widehat{p}_n^{j_1}\phi_n^{j_1}(t) - p^{\sim 0}(t),
\tag{13}
$$

$$
p^{\sim 2}(t) = p(t) - p^{\sim 0}(t) - p^{\sim 1}(t),
\tag{14}
$$

with the notations ~ 0, ~ 1, and ~ 2 signifying respectively the corresponding large-scale, meso-scale, and sub-mesoscale windows. As V_{ϱ,j_0}, W_{ϱ,j_0-j_1}, W_{ϱ,j_1-j_2} are all subspaces of V_{ϱ,j_2}, functions $p^{\sim 0}$ and $p^{\sim 1}$ can be transformed using the spanning basis of V_{ϱ,j_2}:

$$
\widehat{p}_n^{\sim \varpi} = \int_0^\varrho p^{\sim \varpi}(t)\,\phi_n^{j_2}(t)\, dt,
\tag{15}
$$

for windows $\varpi = 0, 1, 2$, and $n = 0, 1, ..., 2^{j_2 \varrho} - 1$, while keeping information only for their corresponding windows. In doing so, the transform coefficients $\widehat{p_n^{\sim\varpi}}$, though discretely defined with n, has the finest resolution permissible in the sampling space on $[0, 1]$. We call (15) a *multiscale window transform*, or MWT for short. With this, (12), (13), and (14) can be written in a unified way:

$$p^{\sim\varpi}(t) = \sum_{n=0}^{2^{j_2 \varrho}-1} \widehat{p_n^{\sim\varpi}} \phi_n^{j_2}(t), \qquad \varpi = 0, 1, 2. \tag{16}$$

Eqs. (15) and (16) form the transform-reconstruction pair for the MWT.

4.2 Marginalization and multiscale energy

As proved in Liang and Anderson (2007), an important Parseval relation-like property of the MWT is

$$\sum_n \widehat{p_n^{\sim\varpi}} \widehat{q_n^{\sim\varpi}} = \overline{p^{\sim\varpi}(t)\, q^{\sim\varpi}(t)}, \tag{17}$$

for $p, q \in V_{\varrho,j_2}$, where the overline indicates an averaging over time, and $\sum_n$ is a summation over the sampling set $\{0, 1, 2, ..., 2^{j_2} - 1\}$. $\sum_n$ is also called "marginalization" as in a localized analysis, properties with locality dependence summed out are usually referred to as marginal properties (see Huang et al., 1999). Eq. (17) states that, a product of two multiscale window transforms followed by a marginalization is equal to the product of their corresponding reconstructions averaged over the duration. We will henceforth refer to it as **property of marginalization**.

The property of marginalization ensures an efficient representation of energy in terms of the MWT transform coefficients. In (17), let $p = q$, the right hand side is then the energy of p (up to some constant factor) averaged over $[0, 1]$. It is equal to a summation of $N = 2^{j_2}$ individual objects $(\widehat{p_n^{\sim\varpi}})^2$ centered at time $t_n = 2^{-j_2}n + \frac{1}{2}$, with a characteristic influence interval $\Delta t = t_{n+1} - t_n = 2^{-j_2}$. The energy represented at time t_n then should be the mean over the interval: $\frac{(\widehat{p_n^{\sim\varpi}})^2}{\Delta t} = 2^{j_2}(\widehat{p_n^{\sim\varpi}})^2$. Note the constant factor 2^{j_2} is essential for physical interpretation. But for notational succinctness, we will neglect it in the following derivations.

5. Canonical transfer with respect to the multiscale window transform

We now carry the canonical transfer (9) to a more generic framework, the MWT framework. Consider again the evolution of a passive scalar T with a governing equation (3). Take an MWT on both sides, and multiply by $\widehat{T_n^{\sim\varpi}}$, the resulting left hand side can be shown to be $\dot{E}_n^\varpi$, time rate of change of the (generalized) multiscale energy (variance) $\frac{1}{2}\left(\widehat{T_n^{\sim\varpi}}\right)^2$. Here ϖ and n represent the window and the time location, respectively. We use a dot to indicate the time rate of change because in performing the transform time t has been translated to the discrete time location n, and hence the time rate of change is actually in an approximate sense. The resulting energy equation is

$$\dot{E}_n^\varpi = -\widehat{T_n^{\sim\varpi}} \nabla \cdot \widehat{(\mathbf{v}T)}_n^{\sim\varpi}, \tag{18}$$

which should be equal to $-\nabla \cdot \mathbf{Q}_n^\varpi + \Gamma_n^\varpi$ for some flux $\mathbf{Q}_n^\varpi$ and transfer Γ_n^ϖ on window ϖ at time step n, based on what we argued before.

Following the same strategy adopted in Liang (2007), we first find $\mathbf{Q}_n^\varpi$, the multiscale flux of $\frac{1}{2}T^2$ by flow $\mathbf{v}$ on window ϖ and time step n. In the MWT framework, it can be obtained through reconstructing the decomposed objects. Notice that

$$\frac{1}{2}T^2 = \sum_{n_1,\varpi_1} \sum_{n_2,\varpi_2} \frac{1}{2}[\widehat{T}_{n_1}^{\sim\varpi_1}\phi_{n_1}^{j_2}(t) \, \widehat{T}_{n_2}^{\sim\varpi_2}\phi_{n_2}^{j_2}(t)], \tag{19}$$

where the summations are over all the possible time steps and windows. We look at the flux of the "atom" $\frac{1}{2}[\widehat{T}_{n_1}^{\sim\varpi_1}\phi_{n_1}^{j_2}(t) \, \widehat{T}_{n_2}^{\sim\varpi_2}\phi_{n_2}^{j_2}(t)]$ by a flow $\mathbf{v}(t)$ (spatial dependence suppressed for clarity) over $t \in [0,1]$ on window ϖ at step n. It is

$$\int_0^1 \mathbf{v}(t) \cdot \frac{1}{2}[\widehat{T}_{n_1}^{\sim\varpi_1}\phi_{n_1}^{j_2}(t) \, \widehat{T}_{n_2}^{\sim\varpi_2}\phi_{n_2}^{j_2}(t)]$$
$$\cdot \delta(n - n_2)\delta(\varpi - \varpi_2) \, dt,$$

where δ is the Kronecker function. [Note the arguments of the δ's can be replaced with $(n - n_1)$ and $(\varpi - \varpi_1)$ without affecting the final result, as all the time steps and window indices are to be summed out.] A flux of $\frac{1}{2}T^2$ by $\mathbf{v}$ on ϖ at n is then the sum of it over all the possible n_1, n_2 and ϖ_1, ϖ_2. By the definition of MWT, this is

$$\mathbf{Q}_n^\varpi = \sum_{n_1,\varpi_1} \sum_{n_2,\varpi_2} \int_0^1 \frac{1}{2}\mathbf{v}(t) \cdot \widehat{T}_{n_1}^{\sim\varpi_1}\phi_{n_1}^{j_2}(t) \cdot \widehat{T}_{n_2}^{\sim\varpi_2}\phi_{n_2}^{j_2}(t)$$
$$\cdot \delta(n - n_2)\delta(\varpi - \varpi_2) \, dt$$
$$= \frac{1}{2}\int_0^1 \mathbf{v}(t)T(t) \cdot \widehat{T}_n^{\sim\varpi}\phi_n^{j_2}(t) \, dt.$$

But $\widehat{T}_n^{\sim\varpi}\phi_n^{j_2}(t)$ lies in window ϖ, and all the windows are mutually orthogonal, so the above equation is equal to

$$\frac{1}{2}\int_0^1 (\mathbf{v}T)^{\sim\varpi} \cdot \widehat{T}_n^{\sim\varpi}\phi_n^{j_2}(t) \, dt.$$

Notice $\widehat{T}_n^{\sim\varpi}$ is a constant with respect to t. Factoring it out and we get, by the definition of MWT,

$$\mathbf{Q}_n^\varpi = \frac{1}{2}\widehat{T}_n^{\sim\varpi}\widehat{(\mathbf{v}T)}_n^{\sim\varpi}. \tag{20}$$

The transfer Γ is obtained by subtracting $-\nabla \cdot \mathbf{Q}_n^\varpi$ from the right hand side of (18):

$$\Gamma_n^\varpi = -\widehat{T}_n^{\sim\varpi}\nabla \cdot \widehat{(\mathbf{v}T)}_n^{\sim\varpi} + \nabla \cdot \left[\frac{1}{2}\widehat{T}_n^{\sim\varpi}\widehat{(\mathbf{v}T)}_n^{\sim\varpi}\right]$$
$$= \frac{1}{2}\left[\widehat{(\mathbf{v}T)}_n^{\sim\varpi} \cdot \nabla\widehat{T}_n^{\sim\varpi} - \widehat{T}_n^{\sim\varpi}\nabla \cdot \widehat{(\mathbf{v}T)}_n^{\sim\varpi}\right]. \tag{21}$$

There is an important property with the transfer thus obtained. Mathematically, it is expressed as

$$\boxed{\sum_n \sum_\varpi \Gamma_n^\varpi = 0.} \tag{22}$$

In fact, by the property of marginalization, (21) gives

$$\sum_n \Gamma_n^\varpi = \frac{1}{2} \int_0^1 \left[(\mathbf{v}T)^{\sim\varpi} \cdot \nabla T^{\sim\varpi} - T^{\sim\varpi} \nabla \cdot (\mathbf{v}T)^{\sim\varpi} \right] \, dt,$$

and because of the orthogonality between different windows, this followed by a summation over ϖ results in

$$\frac{1}{2} \int_0^1 \left[(\mathbf{v}T) \cdot \nabla T - T \nabla \cdot (\mathbf{v}T) \right] \, dt = 0.$$

In the above derivation, the incompressibility assumption of the flow has been used.

Property (22) states that the transfer (21) vanishes upon summation over all the windows and marginalization over the time sampling space. Because of its similarity in form to the Poisson bracket in Hamiltonian mechanics, we will refer it to as *canonical* in the future to distinguish it from other transfers one might have met in the literature. Canonical transfers only re-distribute energy among scale windows, without generating or destroying energy as a whole.

The canonical transfer (21) may be further simplified in expression when $\widehat{T}_n^{\sim\varpi}$ is nonzero:

$$\Gamma_n^\varpi = -E_n^w \, \nabla \cdot \left(\frac{\widehat{(\mathbf{v}T)_n}^{\sim\varpi}}{\widehat{T}_n^{\sim\varpi}} \right), \text{ if } \widehat{T}_n^{\sim\varpi} \neq 0, \tag{23}$$

where $E_n^\varpi = \frac{1}{2} \left(\widehat{T}_n^{\sim\varpi} \right)^2$ is the energy on window ϖ at step n, and is hence always positive. Note that (23) defines a field variable which has the dimension of velocity in physical space:

$$\mathbf{v}_T^\varpi = \frac{\widehat{(T\mathbf{v})_n}^{\sim\varpi}}{\widehat{T}_n^{\sim\varpi}}. \tag{24}$$

It may be loosely understood as a weighted average in time, with the weights derived from the MWT of the scalar field T. For convenience, we will refer to $\mathbf{v}_T^\varpi$ as *T-coupled velocity*. The growth rate of energy on window ϖ is now totally determined by $-\nabla \cdot \mathbf{v}_T^\varpi$, the convergence of $\mathbf{v}_T^\varpi$, and

$$\Gamma_n^\varpi = -E_n^\varpi \nabla \cdot \mathbf{v}_T^\varpi. \tag{25}$$

Note Γ_n^ϖ makes sense even though $\widehat{T}_n^{\sim\varpi} = 0$ and hence $\mathbf{v}_T^\varpi$ does not exist. In this case, (25) should be understood as (21). We may keep using (23) and (25) for notational simplicity and physical clarity.

6. Connection to the formalism with respect to Reynolds decomposition

It is of interest to connect the transfer of (21) to that obtained by Liang (2007) within the framework of Reynolds decomposition, i.e., that of (9), with an ensemble mean understood as a time average. As the Reynolds formalism does not allow for time dependence in Γ, we perform a marginalization on the transforms. A basic property of the MWT is that, when $j_0 = 0$ and a periodic extension is used for the time sequence, the field in a two-window

decomposition is reconstructed to a mean (over time) and the deviation from the mean (see Liang and Anderson, 2007). In that case,

$$
\begin{aligned}
\sum_n \Gamma_n^1 &= \frac{1}{2} \left[\overline{(\mathbf{v}T)' \cdot \nabla T'} - \overline{T' \nabla \cdot (\mathbf{v}T)'} \right] \\
&= \frac{1}{2} \left[\bar{T} \nabla \cdot (\overline{\mathbf{v}'T'}) - (\overline{\mathbf{v}'T'}) \cdot \nabla \bar{T} \right],
\end{aligned}
\tag{26}
$$

where in the derivation, the decomposed version of continuity equation $\nabla \cdot \bar{\mathbf{v}} = 0$ and $\nabla \cdot \mathbf{v}' = 0$ has been used. This is the very Γ in (7). Likewise, $\sum_n \Gamma_n^0$ is the $-\Gamma$ in (6). So the canonical transfer of Liang (2007) is a particular case of the present formalism (21).

7. Interaction analysis

In contrast to the canonical transfer (9) resulting from the Reynolds decomposition, the localized Γ_n^ϖ of (21) involves not only inter-window energy transfers, but also transfers from within the same window. As an instability/stability is by definition a process between different windows, we need to eliminate the information other than the inter-window transfer from the Γ_n^ϖ obtained above. This is achieved through a technique called interaction analysis, which has been used by Liang and Robinson (2005) in the MWT framework to single out the desired processes from quadratic energetic terms.

It is observed in (21) that Γ_n^ϖ is made of terms in the form $\Gamma_{\mathcal{R}pq,n}^\varpi = \widehat{\mathcal{R}}_n^{\sim\varpi} \widehat{pq}_n^{\sim\varpi}$, for $\mathcal{R}, p, q \in V_{\varrho,j_2}$. Using the transform-analysis pair (15) and (16),

$$
\Gamma_{\mathcal{R}pq,n}^\varpi = \sum_{\varpi_1,\varpi_2} \sum_{n_1,n_2} Tr(n,\varpi \mid n_1,\varpi_1; n_2,\varpi_2),
\tag{27}
$$

with the *basic transfer function* of $\Gamma_{\mathcal{R}pq,n}^\varpi$

$$
Tr(n,\varpi \mid n_1,\varpi_1; n_2,\varpi_2) = \widehat{\mathcal{R}}_n^{\sim\varpi} \frac{\widehat{p}_{n_1}^{\sim\varpi_1} \widehat{q}_{n_2}^{\sim\varpi_2} + \widehat{p}_{n_2}^{\sim\varpi_2} \widehat{q}_{n_1}^{\sim\varpi_1}}{2} (\widehat{\phi_{n_1}^{\varrho,j_2} \phi_{n_2}^{\varrho,j_2}})_n^{\sim\varpi}.
\tag{28}
$$

Following the terminology of Iima and Toh (1995), $Tr(n,\varpi \mid n_1,\varpi_1; n_2,\varpi_2)$ represents an interaction between the *receiving mode* (n,ϖ), and *giving modes* (n_1,ϖ_1), and (n_2,ϖ_2). It gives the energy made to the receiving mode from the two giving modes. Here both the index pairs (n_1,ϖ_1) and (n_2,ϖ_2) are dummy in (27). We write in (28) $\frac{1}{2} \left[\widehat{p}_{n_1}^{\sim\varpi_1} \widehat{q}_{n_2}^{\sim\varpi_2} + \widehat{p}_{n_2}^{\sim\varpi_2} \widehat{q}_{n_1}^{\sim\varpi_1} \right]$ instead of $(\widehat{p}_{n_1}^{\sim\varpi_1} \widehat{q}_{n_2}^{\sim\varpi_2})$ to ensure symmetry. Using this definition it is easy to show that the basic transfer function of our canonical transfer Γ_n^ϖ defined in (21) satisfies a detailed balance relation which is found in interaction analyses in a variety of contexts (cf. Lesieur 1990, Pope 2003). See Appendix 13 for details.

Every transfer can now be viewed as an installment of the basic transfer functions. The purpose of interaction analysis is to extract the cross-window transfer from these functions. For instability analysis, particularly, we need to find the transfer from the mean window (or window 0) to the eddy window (or window 1) in a two-window decomposition. For example, if we are dealing with $\Gamma_{\mathcal{R}pq,n}^1 = \widehat{\mathcal{R}}_n^{\sim 1} \widehat{(pq)}_n^{\sim 1}$, the summation in (27) over $\varpi_1, \varpi_2, n_1, n_2$ organizes the product pq into four parts (see Liang and Robinson, 2005):

$$
p^{\sim 0}q^{\sim 0}, \quad p^{\sim 0}q^{\sim 1}, \quad p^{\sim 1}q^{\sim 0}, \quad p^{\sim 1}q^{\sim 1}.
$$

The last part $p^{\sim 1}q^{\sim 1}$, while combined with $\widehat{\mathcal{R}}_n^{\sim 1}$, gives the energy transferred within the eddy window. So it must be removed if only stability/instability is concerned. Using superscript $0 \to 1$ to signify an operator that selects out the transfer from window 0 to window 1, we have

$$\left(\Gamma_{\mathcal{R}pq,n}^1\right)^{0\to1} = \widehat{\mathcal{R}}_n^{\sim 1}\left((\widehat{p^{\sim 0}q^{\sim 0}})_n^{\sim 1} + (\widehat{p^{\sim 0}q^{\sim 1}})_n^{\sim 1} + (\widehat{p^{\sim 1}q^{\sim 0}})_n^{\sim 1}\right). \tag{29}$$

This operator can be easily applied to the canonical transfer. For example, an application to (21) with $\varpi = 1$ gives

$$(\Gamma_n^1)^{0\to1} = \frac{1}{2}\left\{\nabla\widehat{T}_n^{\sim 1}\cdot\left[(\widehat{\mathbf{v}^{\sim 0}T^{\sim 0}})_n^{\sim 1} + (\widehat{\mathbf{v}^{\sim 0}T^{\sim 1}})_n^{\sim 1} + (\widehat{\mathbf{v}^{\sim 1}T^{\sim 0}})_n^{\sim 1}\right]\right.$$
$$\left. - \widehat{T}_n^{\sim 1}\nabla\cdot\left[(\widehat{\mathbf{v}^{\sim 0}T^{\sim 0}})_n^{\sim 1} + (\widehat{\mathbf{v}^{\sim 0}T^{\sim 1}})_n^{\sim 1} + (\widehat{\mathbf{v}^{\sim 1}T^{\sim 0}})_n^{\sim 1}\right]\right\}. \tag{30}$$

8. Hydrodynamic stability analysis

Hydrodynamic stability usually concerns with the transfer process between two windows, the large-scale window and the eddy window. But sometimes the transfer to a smaller scale window, e.g., a turbulence window, might also be of interest. In this section, we first give the instability identification criterion with a two-window decomposition, then in section 8.4 briefly touch the formalism with three windows.

8.1 Idealized flow
We proceed to find the criterion for instability. For an ideal (frictionless) incompressible fluid flow, the governing equations are

$$\frac{\partial\mathbf{v}}{\partial t} = -\nabla\cdot(\mathbf{v}\mathbf{v}) - \frac{\nabla P}{\rho}, \tag{31}$$

$$\nabla\cdot\mathbf{v} = 0. \tag{32}$$

Here we do not consider the acceleration of gravity; thus only kinetic energy is involved. This is useful in practice unless buoyancy is perturbed. Following the procedure in section 5, it is easy to know that the pressure term makes no contribution to the energy transfer across scale windows in an incompressible flow. Actually, an MWT of (31) followed by a dot product with $\widehat{\mathbf{v}}_n^{\sim 1}$ results in a pressure working rate proportional to $\widehat{\mathbf{v}}_n^{\sim 1}\cdot\nabla\widehat{P}_n^{\sim 1}$, which is equal to $\nabla\cdot\left(\widehat{P}_n^{\sim 1}\widehat{\mathbf{v}}_n^{\sim 1}\right)$ by the MWTed continuity equation. Only the nonlinear terms require some thought for the canonical transfer.

Let the scalar T in (25) be u, v, w. We have a u-coupled velocity, a v-coupled velocity, and a w-coupled velocity, and hence a canonical transfer on the eddy window:

$$\Gamma_n^1 = -\frac{1}{2}\left[(\widehat{u}_n^{\sim 1})^2\nabla\cdot\mathbf{v}_u^1 + (\widehat{v}_n^{\sim 1})^2\nabla\cdot\mathbf{v}_v^1 + (\widehat{w}_n^{\sim 1})^2\nabla\cdot\mathbf{v}_w^1\right].$$

This is well-defined even when the coupled velocities vanish. In that case, one only needs to do an expansion with the above equation. Applying the interaction analysis to select out the process from window 0 to window 1, the expanded equation results in a metric

$$\mathcal{P}_{\mathbf{x},n} = \left(\Gamma_n^1\right)^{0\to1} = -\frac{1}{2}\left[\widehat{(\mathbf{v}\mathbf{v})}_n^{\sim 1}:\nabla\widehat{\mathbf{v}}_n^{\sim 1} - \nabla\cdot\widehat{(\mathbf{v}\mathbf{v})}_n^{\sim 1}\cdot\widehat{\mathbf{v}}_n^{\sim 1}\right]^{0\to1} \tag{33}$$

Based on the argument in the foregoing sections, a localized stability criterion consistent with the Lyapunov definition is naturally obtained:

The system under consideration is

(i) stable at $(\mathbf{x}, n)$ if $\mathcal{P}_{\mathbf{x},n} < 0$;

(ii) unstable otherwise, and

(iii) the (algebraic) growth rate is $\mathcal{P}$.

This stability criterion is stated with $\mathcal{P}$ in the form of a spatio-temporal field, albeit the time dependence is discrete (n), in contrast to the bulk form in the original Lyapunov definition.

8.2 Real fluids

For a real fluid flow, one generally needs to take into account more physical effects in the governing equations. Buoyancy, dissipation, compressibility, for example, may not be negligible in many cases. As different problems usually have different governing equations, it is not our intention in this study to give a universal expression of the localized stability criterion. We just present the general strategy to obtain the metric.

The commonality of these factors is that they usually do not involve nonlinear interaction in the multiscale energetics, so it is generally easy to incorporate their inputs into our formulation. The key is to have the transport singled out, which is straightforward should there be only linear processes. If buoyancy is perturbed, then potential energy must be counted in. In that case, the system stability is dependent on the growth of perturbation mechanic energy (kinetic energy plus potential energy), instead of just kinetic energy alone.

As an example, we show how this works when dissipation is included in (31). We choose this example not just because of its ubiquity, but also because it will be needed in an application later on.

Dissipation appears in Eq. (31) as an extra term $\nabla \cdot (\nu \nabla \mathbf{v})$. In forming the energetics for window 1, this term results in

$$\widehat{\mathbf{v}}_n^{\sim 1} \cdot \nabla \cdot (\nu \nabla \widehat{\mathbf{v}}_n^{\sim 1}) = \nabla \cdot (\nu \nabla \widehat{\mathbf{v}}_n^{\sim 1} \cdot \widehat{\mathbf{v}}_n^{\sim 1}) - \nu \nabla \widehat{\mathbf{v}}_n^{\sim 1} : \nabla \widehat{\mathbf{v}}_n^{\sim 1}.$$

So the instability criterion metric now should be Eq. (33) plus the non-transport part on the right hand side of the above equation:

$$\begin{aligned}
\mathcal{P}_{\mathbf{x},n} &= -\frac{1}{2}\left[\widehat{(\mathbf{vv})}_n^{\sim 1} : \nabla \widehat{\mathbf{v}}_n^{\sim 1} - \nabla \cdot \widehat{(\mathbf{vv})}_n^{\sim 1} \cdot \widehat{\mathbf{v}}_n^{\sim 1} \right]^{0 \to 1} - \nu \nabla \widehat{\mathbf{v}}_n^{\sim 1} : \nabla \widehat{\mathbf{v}}_n^{\sim 1} \\
&= -\frac{1}{2}\left[\left(\widehat{(\mathbf{vv})}_n^{\sim 1} + 2\nu \nabla \widehat{\mathbf{v}}_n^{\sim 1} \right) : \nabla \widehat{\mathbf{v}}_n^{\sim 1} - \nabla \cdot \widehat{(\mathbf{vv})}_n^{\sim 1} \cdot \widehat{\mathbf{v}}_n^{\sim 1} \right]^{0 \to 1}
\end{aligned} \quad (34)$$

The dissipative input in $\mathcal{P}_{\mathbf{x},n}$ always appears negative; it thus functions to reduce the local energy transfer, as is expected. On the other hand, because of its localized feature, it might modify the stability metric distribution, and hence lead to the emergence of some new stability pattern.

8.3 Instability identification from a large-scale point of view

The above criterion is established based on the eddy window or window 1. Instability can also be described from a large-scale point of view. This makes sense as a canonical transfer is a protocol between two scale windows: If the eddy window works, we may as well equally view the problem from the large-scale window. The advantage of a large-scale formulation is

to have the eddy scale features filtered, for the transfer thus derived is on the balance of the large-scale energetics. For an idealized fluid, we may define:

$$\mathcal{P}_{\mathbf{x},n} = +\frac{1}{2}\left[\widehat{(\mathbf{vv})}_n^{\sim 0} : \nabla\widehat{\mathbf{v}}_n^{\sim 0} - \nabla\cdot\widehat{(\mathbf{vv})}_n^{\sim 0}\cdot\widehat{\mathbf{v}}_n^{\sim 0}\right]^{1\rightarrow 0}. \tag{35}$$

Notice the positive sign here, compared to the negative sign in (33), as in this case, a positive Γ_n^0 is toward the large-scale window. Also notice the different interaction analysis operator $1 \rightarrow 0$. Eqs. (35) and (33) are equivalent on the large-scale window because the transfer is canonical. This can be easily proved with the definition of canonical transfer (22).

For real fluids, the problem is not as simple as that in the preceding subsection: The canonical transfer and other terms to be combined are not defined on the same scale window. To circumvent the difficulty, we first take averaging for the extra eddy scale energetic terms over an interval in the sampling space commensurate with the large-scale window transform, before adding these terms to the canonical transfer. As an example, consider the dissipative case. The metric in (35) now becomes

$$\mathcal{P}_{\mathbf{x},n} = +\frac{1}{2}\left[\widehat{(\mathbf{vv})}_n^{\sim 0} : \nabla\widehat{\mathbf{v}}_n^{\sim 0} - \nabla\cdot\widehat{(\mathbf{vv})}_n^{\sim 0}\cdot\widehat{\mathbf{v}}_n^{\sim 0}\right]^{1\rightarrow 0} - \nu\overline{\nabla\widehat{\mathbf{v}}_\ell^{\sim 1}:\nabla\widehat{\mathbf{v}}_\ell^{\sim 1}}, \tag{36}$$

where the averaging over ℓ is taken in the sampling space over interval $[n - 2^{j_2-j_0-1}, n + 2^{j_2-j_0-1}]$. The instability identification criterion with $\mathcal{P}$ is the same as that stated in the previous subsections. When other effects are taken into account, $\mathcal{P}$ can be defined likewise as it is defined in (36).

8.4 Mean-eddy-turbulence interaction

Sometimes just two scale windows are not enough to characterize the fluid processes. For instance, one often encounters problems involving interactions between mean, eddy, and turbulent windows. In that case, a system could not only lose stability to fuel the growth of the eddy events, but also transfer energy from the eddy window to the turbulence window through another instability.

We remark that this situation is in fact already taken into account in the formalism of canonical transfer. By (21) it is easy to obtain

$$\Gamma_n^\varpi = -\frac{1}{2}\left[\widehat{(\mathbf{vv})}_n^{\sim\varpi} : \nabla\widehat{\mathbf{v}}_n^{\sim\varpi} - \nabla\cdot\widehat{(\mathbf{vv})}_n^{\sim\varpi}\cdot\widehat{\mathbf{v}}_n^{\sim\varpi}\right] \tag{37}$$

for the governing equations (31) and (32). Different instability metric can be formed by taking the interaction analysis. For example, $\left(\Gamma_n^2\right)^{1\rightarrow 2}$ and $\left(\Gamma_n^2\right)^{0\rightarrow 2}$ represent, respectively, the transfer from the eddy window to the turbulence window, and the transfer from the mean window directly to the turbulence window.

9. Application to oceanographic studies

The above theory and methodology have been applied to problems in different fields in fluid dynamics, such as oceanography, turbulence, fluid control, to name a few. In this section we briefly summarize the results of Liang and Robinson (2009) on a successful application to the dynamical interpretation of a rather complicated ocean phenomenon, the Monterey Bay circulation.
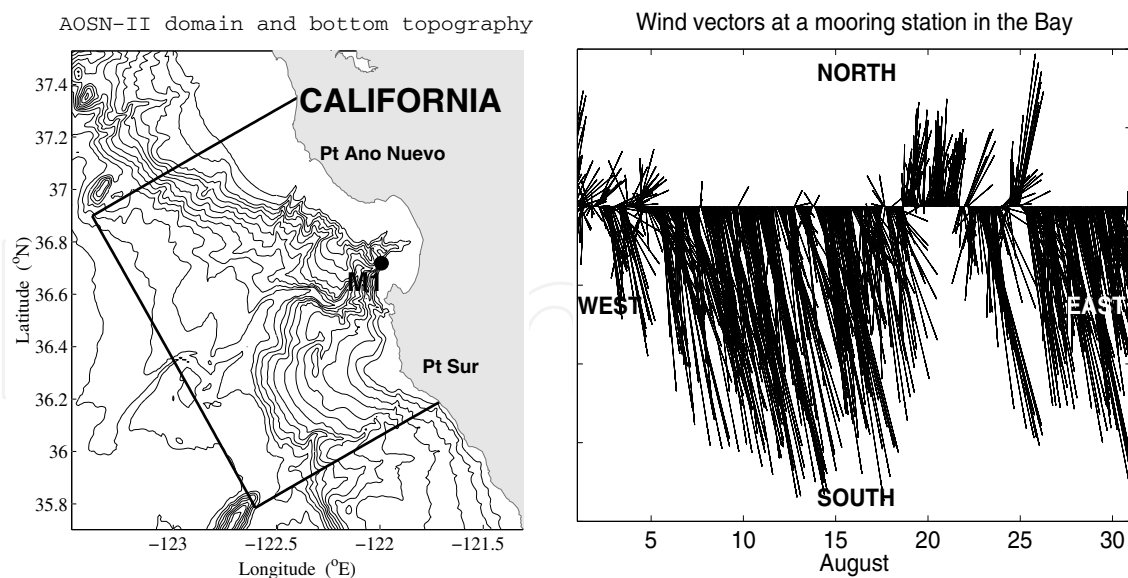
Fig. 2. Left: The research domain and bottom topography of Monterey Bay and its adjacent regions for the August 2003 AOSN-II Experiment. Also shown is the location of a mooring station (M_1) within the Bay. Right: The wind vectors in August 2003 at Station M_1.

Monterey Bay is a large embayment located to the south of San Francisco, California (Fig. 2). Distinguished by its high productivity and marine life diversity, it has been arousing enormous interest in the oceanographic community (see Liang and Robinson, 2009, and references therein). Among the existing issues, how the Monterey Bay circulation is excited and sustained has been of particular interest ever since the 1930s, which had been a continuing challenge until a breakthrough was made recently by Liang and Robinson (2009), with the aid of the afore-mentioned new machinery namely the multiscale window transform (MWT), and an earlier version of the MWT-based stability analysis tailored for atmosphere-ocean problems (Liang and Robinson, 2007). In their study, Liang and Robinson (2009) examined an unprecedented dataset acquired in August 2003 during the Second Autonomous Ocean Sampling Network (AOSN-II) Experiment, a program with the involvement of more than 10 major institutions nationwide in the United States. Out of the observational data the 4D flow field is reconstructed in an optimal way for the duration in question using the Harvard Ocean Prediction System (Haley et al., 2009). Shown in Fig. 3 are several snapshots of the surface flow. As expected, it looks very complex; there seems to be no way to dynamically interpret it with the geophysical fluid dynamics (GFD) theories available then.

Cherishing the hope that underlying the seemingly chaotic phenomena the dynamical processes could be tractable, let us look at the canonical transfers and their evolutions. To do this, first we need to determine the scale windows where the respective processes occur. This is fulfilled by analyzing the wavelet spectra of some typical time series. Shown in Fig. 4 is such a series and its spectrum. Note here we have to use orthonormal wavelets to allow for a definition of energy in the physical sense (see Liang and Anderson, 2007). By observation there is a clear gap between scale levels 2 and 3; accordingly j_0 is chosen to be 2, which corresponds to a time scale of $2^{-j_0} \times$ duration $= 2^{-2} \times 32 = 8$ days. Likewise, a reasonable choice for j_1 is 5, corresponding to a time scale of 1 day. (This essentially keeps the mesoscale window free of tides.) With these parameters, the canonical transfers and hence the stability criterion can be computed in a straightforward way. In Liang and Robinson (2007), we have established that here the criterion actually corresponds to that for the barotropic
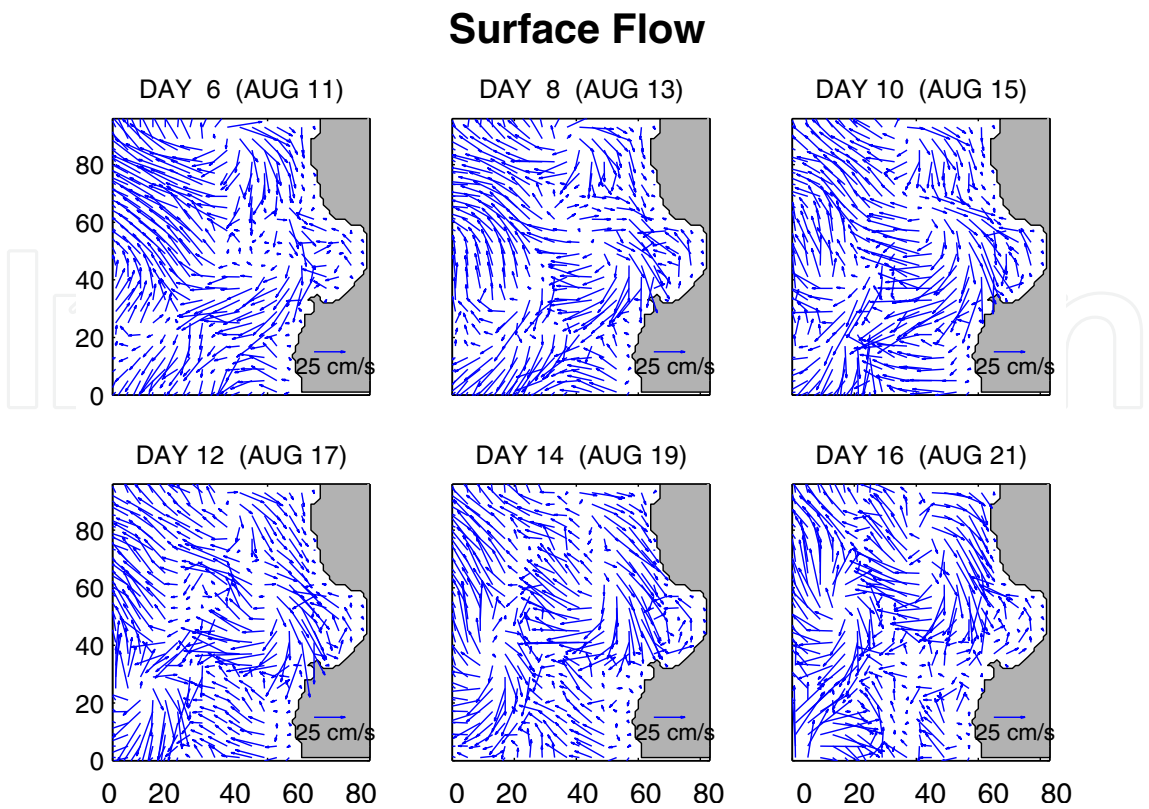
Surface Flow

Fig. 3. Snapshots of the surface flow reconstructed from the 2003 AOSN-II dataset. The domain in Fig. 2 has been rotated by $30^{°}$ clockwise.
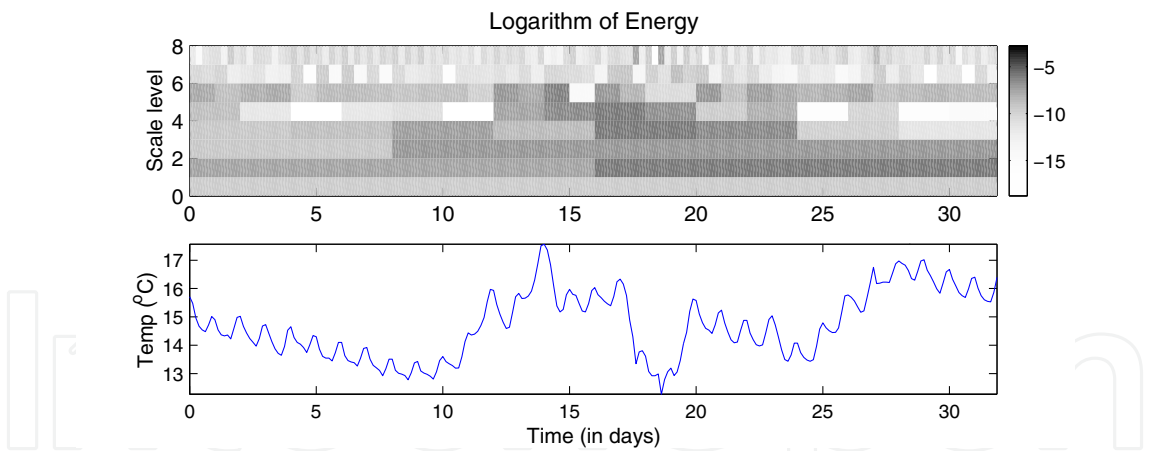

Fig. 4. A time series of the surface temperature at a point off Pt. Ano Nuevo (lower panel) and its orthonormal wavelet spectrum (upper panel). In performing the spectral analysis, the mean has been removed for clarity.

instability in GFD. For convenience in this context, we write it as BT. Meanwhile, In (23), replacing T by density anomaly ρ we get the canonical potential energy transfers. We are particularly interested in the transfer from window 0 to window 1 which, if the interaction analysis operator $0 \rightarrow 1$ is applied, has been proved to correspond to the baroclinic instability identification criterion in GFD (Liang and Robinson, 2007). We shorthand it as BC henceforth. Surprisingly, though the flow is very chaotic, both BT and BC follow a similar and quite regular evolutionary pattern. Contoured in Fig. 5 are the 10-meter BCs at several time instants.
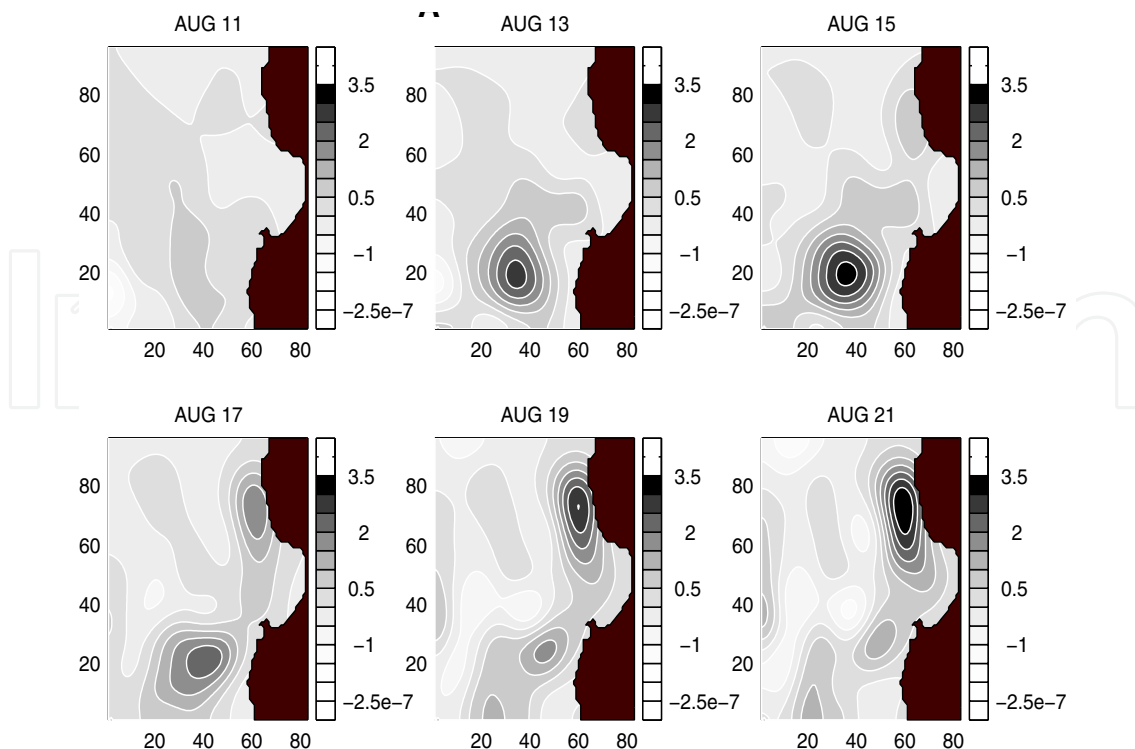
Fig. 5. A time sequence of the 10-meter BC (units: m^2/s^3). Positive values indicate baroclinic instability.

Clearly there are two centers of instability, the northern one lying off Pt. Ano Nuevo, another off Pt. Sur. Generally, during the experimental period, the former gets strengthened as time moves on, while the latter varies the opposite way. Comparing to the wind vectors (Fig. 2), when the northwesterly (southeastward), i.e., the upwelling-favorable wind, prevails, an instability (baroclinic and barotropic) occurs off Pt. Sur; when the wind is relaxed, the Pt. Sur instability disappears, but the relaxation triggers another instability off Pt. Ano Nuevo. This instability is also baroclinic and barotropic, i.e., mixed, in nature. Liang and Robinson (2009) showed that this bimodal structure supplies two sources of mesoscale processes. The resulting mesoscale eddies propagate northward in the form of coastal-trapped waves, with a celerity of about 0.09 m/s. It is the mesoscale activities that make the flow pattern complex.

The above discovery is remarkable; it shows that, during the AOSN-II experimental period, large-scale winds actually do not directly excite the Monterey Bay region circulation, in contrast to predictions with classical theories. Rather, it stores energy in the large-scale window, and then release to the mesoscale window through baroclinic and barotropic instabilities. The mesoscale disturbances are organized in the form of eddies, which, once formed, propagate northward as coastal-trapped waves. Liang and Robinson (2009) also found that a significant upwelling event in this region is driven through nonlinear instabilities, distinctly different from the classical coastal upwelling paradigm.

10. Application to turbulence structure studies

The above theory and methodology have also been applied to turbulence research. Here we briefly summarize the study by Liang and Wang (2004) with a benchmark simulation of a saturated turbulent wake behind a circular cylinder (Reynolds number: Re=3900). The
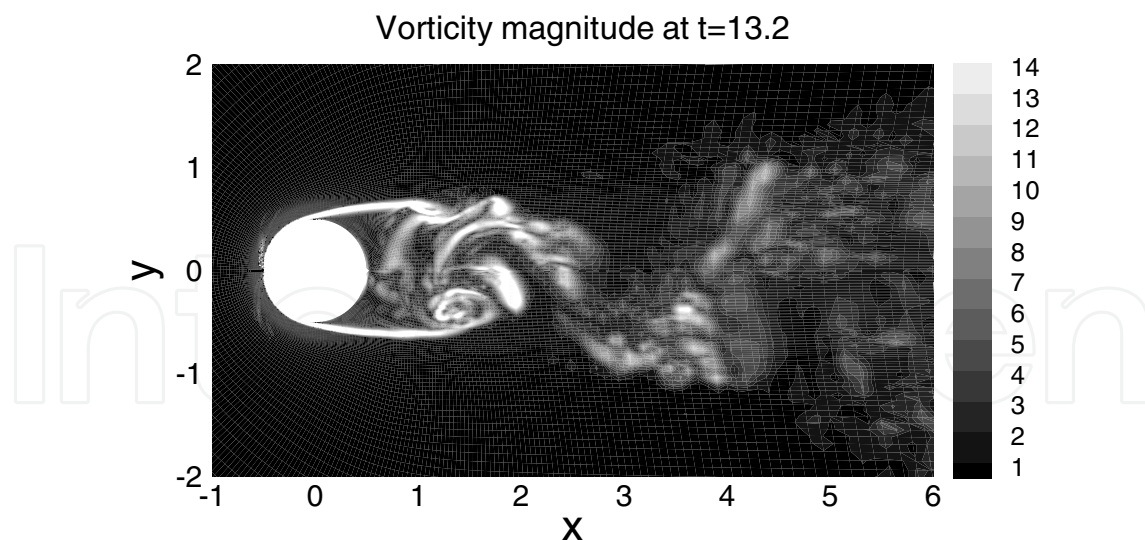
Fig. 6. A saturated turbulent wake at Re=3900 (from Liang and Wang, 2004). Shown here is the vorticity magnitude on a spanwise plane at $t = 13.2$ (arbitrary starting time after a statistical equilibrium).

configuration is referred to Fig. 6, with x, y, and z indicating the streamwise, cross-stream, and spanwise coordinates, respectively ((x, y) originated at the cylinder center). The variables are nondimensionalized with the cylinder diameter d as the length scale, free-stream velocity U_∞ as the velocity scale, and d/U_∞ as the time scale. The dataset for analysis is generated using an energy-conserving, hybrid finite-difference/spectral model, as described in Mittal and Moin (1997). Incompressible Navier-Stokes equations are solved on a C-type mesh using a numerical scheme with second-order central differences in the streamwise and cross-stream directions, and Fourier collocation in the spanwise direction. The subgrid processes are parameterized with the dynamical model described in Germano et al. (1991) and Lilly (1992). The time advancement is of the fractional step type in combination with the Crank-Nicholson method for viscous terms and third order Runge-Kutta scheme for the convective terms. The resulting Poisson equation for pressure is solved using a multigrid iterative procedure at each Runge-Kutta substep. More details about the numerics are referred to Liang and Wang (2004). Shown in Fig. 6 is a snapshot of the computed instantaneous vorticity magnitude.

To perform stability analysis for the simulation, we first determine the scale window bounds. This is fulfilled through orthonormal wavelet spectral analysis. The needed time series are chosen from the velocity components at several typical points within the wake. Following the same procedure as for the above oceanographic problem, it is justified that $j_0 = 1$ and $j_1 = 2$, together with a symmetric extension, serve our purpose well. Shown in Fig. 7 is the multiscale decomposition of a typical time series–the time series of of u at point $(2, -0.5, 0)$. On the right hand side of the equality are the large-scale, mesoscale, and sub-mesoscale reconstructions. Generally, turbulence problems involve complicated scale window structures. Here the mesoscale window is characterized by amplifications of vortex shedding processes, and the process within the sub-mesoscale window appears turbulent.

We now investigate the window interactions with the above theory on localized hydrodynamic stability. As before, we continue to analyze from a longer-time span point of view. That is to say, we will use (36) rather than (34) for the analysis. The results are presented in a spanwise plane only, albeit the analysis is three-dimensional. This is justified by the fact that in a statistical sense the flow field is equivalent spanwise.
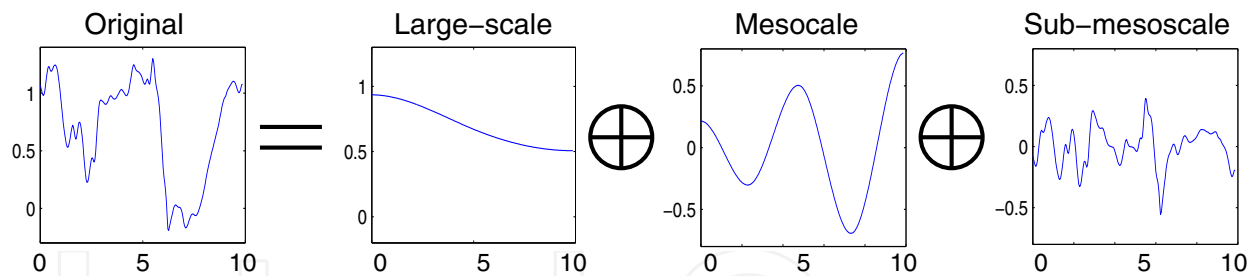
Fig. 7. Multiscale window decomposition of the time series of u at point $(2, -0.5, 0)$. Window bounds used are $j_0 = 1$, and $j_1 = 2$. The abscissa and ordinate are time (scaled by d/U_∞) and u (scaled by U_∞), respectively.
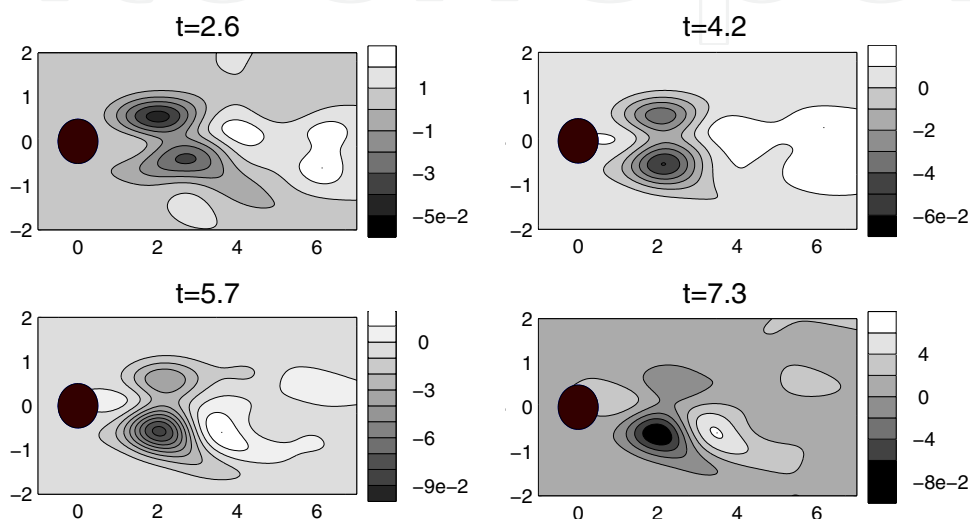

Fig. 8. The canonical kinetic energy transfer from the mesoscale window to the large-scale window for the saturated turbulent wake (adapted from Liang and Wang, 2004). Negative values (in black) indicate instability. The abscissa and ordinate are x and y, respectively.

Figure 8 is the canonical kinetic energy transfer from the meso-scale window to the large-scale window originally computed by Liang and Wang (2004). It differs from (36) by a minus sign; that means here negative values indicate instability. From it obviously there are two centers of instability, each located at one side of the x-axis. These centers are permanent, though their magnitudes do oscillate with time. In the episode as shown, the oscillations are out of phase. The transfer center on the top flank weakens as time goes on, while on the bottom the transfer strengthens. Another observation is that, some inverse transfers (white regions in the figure) are found in the near and far wake, or sandwiched between the instability lobes.

It is these two centers of hydrodynamic instability that cause the shedding of the vortices. This, however, does not correspond to what one may observe about the perturbation growth in vortex shedding. Indeed, by computation both the maximal disturbance and the largest disturbance growth are in the near wake along the x-axis (e.g., Liang, 2007). The discrepancy in location between instability and disturbance growth reveals a fundamental fact in fluid dynamics which has been mostly overlooked: Rapid amplification of perturbation does not necessarily correspond to instability; the eddy energy, when generated, may be transported away instantaneously and lead the perturbation to grow elsewhere. From our results, this observation is in fact a rule rather than an exception. In other words, the causality of
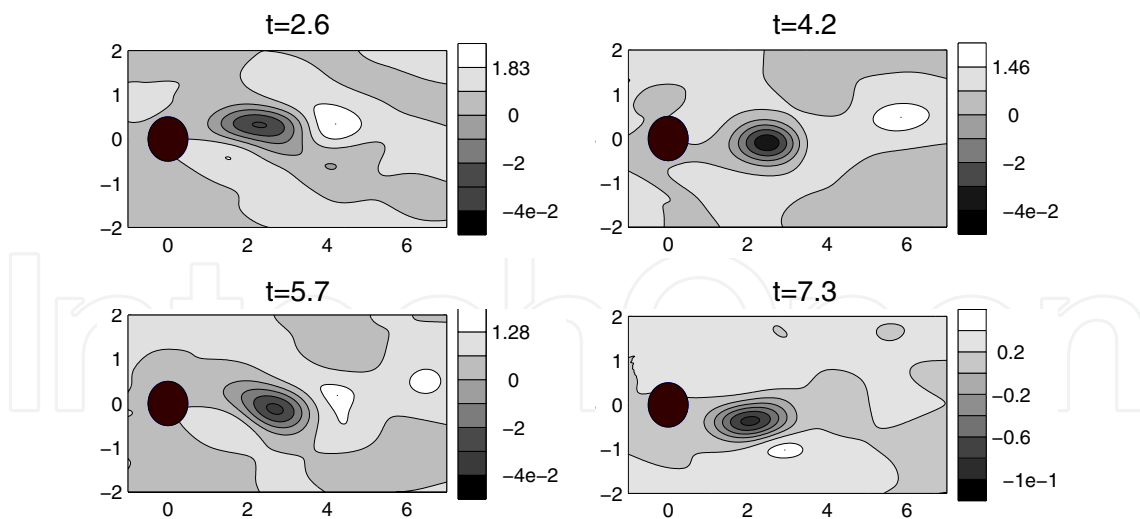
Fig. 9. As Fig. 8, but for the transfer from the sub-mesoscale window to the mesoscale window (adapted from Liang and Wang, 2004).

perturbation growth is usually not local; what we have observed by visual inspection may not reflect the underlying dynamical processes.

The above is about the canonical transfer between the large-scale window and the mesoscale window. We go on to investigate that between the mesoscale and sub-mesoscale windows. In the decomposition in Fig. 7, we have seen that this accounts for how turbulence is produced. As above, the analysis is performed from the stance on the mesoscale window, instead of the sub-mesoscale window, to ensure a better understanding of the dynamics on a longer time span. The result on a spanwise plane is contoured in Fig. 9. Again, this is what was originally obtained by Liang and Wang (2004), and differ from our previous instability metric by a negative sign. That is to say, in the figure negative values (in black) imply instability. Notice that here the canonical transfer is mainly within a monopole lying near the x-axis, in contrast to the dipole structure in Fig. 8. This is interesting, for it shows that the energy gained by the mesoscale process from the basic flow does not go directly to the sub-mesoscale window where the turbulent structures reside. Instead, it is first transported from the two side lobes to the center and then released to fuel the turbulence. As in Fig. 8, inverse transfers are found in the far wake, indicating that some re-laminarization is occurring there.

The instability structures in Figs. 8 and 9 indicate that, in a saturated turbulent wake, there are two primary instabilities, either on one side of the x-axis, followed by a secondary instability lying in between on the axis. The primary instabilities form the mechanism for the vortex shedding; the secondary instability derives the energy from the mesoscale window and funnels energy to sustain the turbulence. These processes are summarized and schematized in Fig. 10.

11. Discussion and conclusions

A localized hydrodynamic stability analysis was developed to relate stability theory to experimental data and direct observations of nature, which are in general highly nonlinear and intermittent in space and time. The theory was applied to the study of the wake behind a circular cylinder, and the suppression of the vortex street formation.

We established that the Lyapunov definition of hydrodynamic stability is essentially about the energy transfer between the mean and eddy states. A transfer is a nonlinear process in
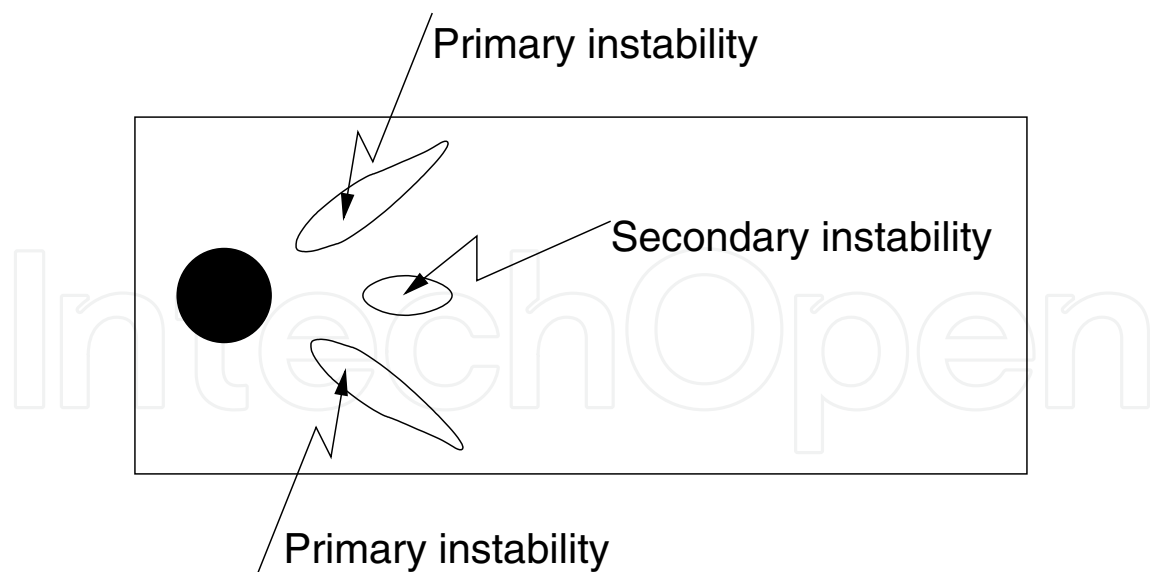
Fig. 10. A schematic of the instability structure in a turbulent wake. The basic flow loses energy to the mesoscale window to shed vortices via the two primary instabilities, while the turbulent processes derive their energy from the vortices through a secondary instability lying in between.

a flow which does not generate nor destroy energy as a whole. In the text it is referred to as "canonical transfer", in distinction from other transfers one may have encountered in the literature. A hydrodynamic instability analysis is thus fundamentally a problem of finding the canonical transfer.

The canonical transfer has been rigorously formulated within the framework of a function analysis apparatus newly developed by Liang and Anderson (2007), i.e., the multiscale window transform, or MWT for short. The MWT is a generalization of the classical mean-eddy decomposition, representing a signal on subspaces or scale windows with distinct time scale ranges. We particularly introduced a large-scale window, a mesoscale window, plus a sub-mesoscale window when needed. Symbolically they are denoted as $\varpi = 0, 1, 2$ for notational convenience. In special cases, these windows may also be referred to as mean window, eddy window, and turbulence window, respectively. The basic idea of the formulation is that the nonlinear process in a flow can be uniquely decomposed into a transport (expressed in a divergence form) and a canonical transfer; if the former is found, the latter follows accordingly. The resulting canonical transfer has a concise form in expression in terms of MWT. In the case of a passive scalar T advected by an incompressible flow, the energy transferred to window ϖ can be written as $\Gamma_n^\varpi = -E_n^\varpi \nabla \cdot \mathbf{v}_T$, where E_n^ϖ is the energy on window ϖ, $\mathbf{v}_T = \frac{\widehat{(\mathbf{v}T)}_n^{\sim\varpi}}{\widehat{T}_n^{\sim\varpi}}$, and $\widehat{(\cdot)}_n^{\sim\varpi}$ indicates an MWT on window ϖ. The complicated multiscale window interaction (mean-eddy-turbulence interaction in particular) in fluid flows is therefore nicely characterized by this concise formula, as schematized in Fig. 11.

Hydrodynamic instability is a particular case of the above multiscale window interaction. Take a two-window decomposition, and consider the eddy window $\varpi = 1$. It is shown that the energy transferred from the background to fuel the variance of T is $\Gamma_n^1 = -E_n^1 \nabla \cdot \mathbf{v}_T$. The instability is then totally determined by the convergence of $\mathbf{v}_T$, a velocity weighted by T in the MWT framework. The same derivation applies to the momentum equations, and a metric $\mathcal{P}$ for hydrodynamic instability can be easily obtained. Note that the so-obtained $\mathcal{P}$ is
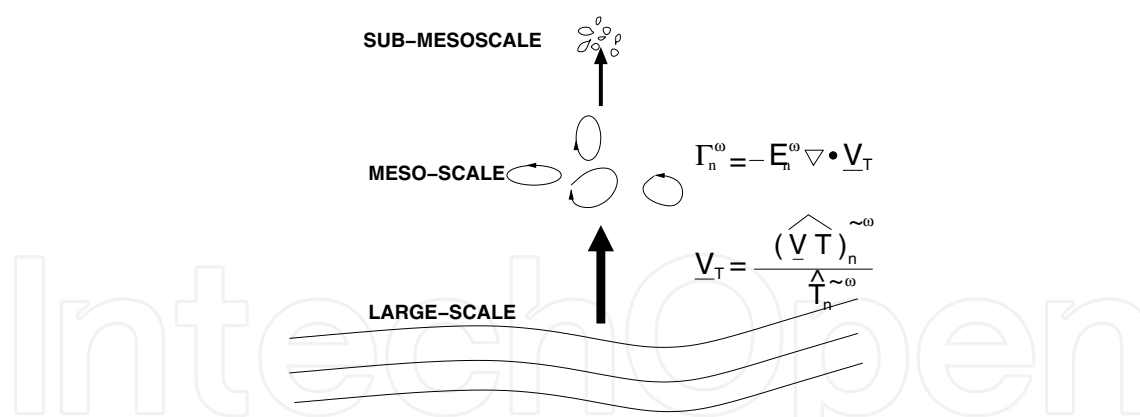
Fig. 11. A schematic of the multiscale window interaction in fluid flows. The intricate multiscale window interaction, and mean-eddy-turbulence interaction in particular, is characterized by a quantity namely the canonical transfer Γ_n^ω (for scale window ϖ and time step n) which, in terms of multiscale window transform, can be succinctly written in a form as Eq. (23) or Eq. (21).

a spatio-temporal field, and hence localized events are naturally represented. For a flow, one can conveniently identify the instability structure, and the corresponding growth rate, simply by visual inspection.

With this convenience we examined an oceanographic problem. For nearly 70 years, how the complex circulation in the Monterey Bay, California, is excited has been a continuing challenge in physical oceanography. Numerous efforts have been invested to investigate its dynamical origins without much luck. This problem, however, becomes straightforward in our framework. With an unprecedented dataset collected in 2003, it is found that, though the circulation seems to be chaotic, the underlying dynamical processes turn out to be tractable. More specifically, the complexity is mainly due to two mixed instabilities which are located outside Pt. Sur and Pt. Ano Nuevo, respectively. The resulting mesoscale eddies propagate northward in the form of coastally trapped waves, orchestrating into a flow complex in pattern. In this study, we see how winds may instill energy into the ocean, first stored in the large-scale window, then releasing to fuel the mesoscale eddies through barotropic and baroclinic instabilities. We have also seen that intense upwelling events may not be directly driven by winds, nor by topography variation, but may have their origin intrinsically embedded in the nonlinearity of the system. These dynamical scenarios are distinctly different from their corresponding classical paradigms.

We have also examined a turbulent wake behind a circular cylinder. It is found the processes are organized into three distinct scale windows: On the two extremes are the basic flow and the turbulence; lying in between are the shedding vortices. The vortex shedding is sustained through two instabilities either on a side of the x-axis, and the mesoscale shedding further releases energy into the sub-mesoscale window to produce turbulence. The former two are what we call primary instabilities, while the latter is a secondary instability. The locations of the instabilities are relatively steady. The primary instabilities are within two lobes, one at a side of the axis; the secondary instability is in the form of a monopole, located mainly along the axis, as shown in Fig. 10. This structure implies that the canonical energy transfer may not be local. In this case, for example, the energy acquired during the primary instabilities must be first transported from the two side lobes to the middle before being utilized for turbulence production. This nonlocal transfer may also be reflected in the discrepancy between perturbation growth and its corresponding canonical transfer. That is to

say, what one sees about the growth at one location may have its origin elsewhere. From the mathematical expressions shown in this study this phenomenon is actually a rule rather than an exception.

The nonlocality of energy transfer raises an issue about causality and accordingly poses a challenge to turbulence simulation in the parameterization of subgrid processes. Since the rapid amplification of perturbation need not be instability, schemes based solely on local perturbation or perturbation growth may not serve the modeling purpose well. We hope the notion of canonical transfer may come to help in this regard.

On both the primary and secondary instability maps for the turbulent wake, a remarkable feature is the inverse transfer spots/centers sandwiched between the instability structures. This phenomenon tells that, even though the flow is turbulent, there exist processes which introduce orders rather than chaos to the system. This phenomenon has profound implications; we look at how it may be utilized for flow control, particularly turbulence control. Turbulence control is an important applied field which has been widely investigated. Several reviews can be found in Huerre and Monkewitz (1990), Oertel (1990), Williamson (1996), Pastoor et al. (2008), to name a few. Generally speaking, to control turbulence is to inhibit perturbation energy from being generated, and accordingly, the traditional control is designed based on suppression of turbulence growth. This goes back to what we have observed above: *Looking solely at the turbulence growth could be misleading, as energy increase does not necessarily occur in accordance with transfer.* Particularly, in a region with perturbation growing there could be actually an ongoing inverse transfer or laminarization lying beneath. If one puts a control in this region to inhibit the perturbation growth, he probably also defeats the laminarization which is actually helpful to control. To illustrate, consider a two-point system as shown in Fig. 12. We have points 1 and 2, with eddy energies K_1^{eddy} and K_2^{eddy}, respectively. Both K_1^{eddy} and K_2^{eddy} grow, but their sources of growth are different. The former is from the *in situ* large-scale window through instability ($\Gamma_1 > 0$), while the latter
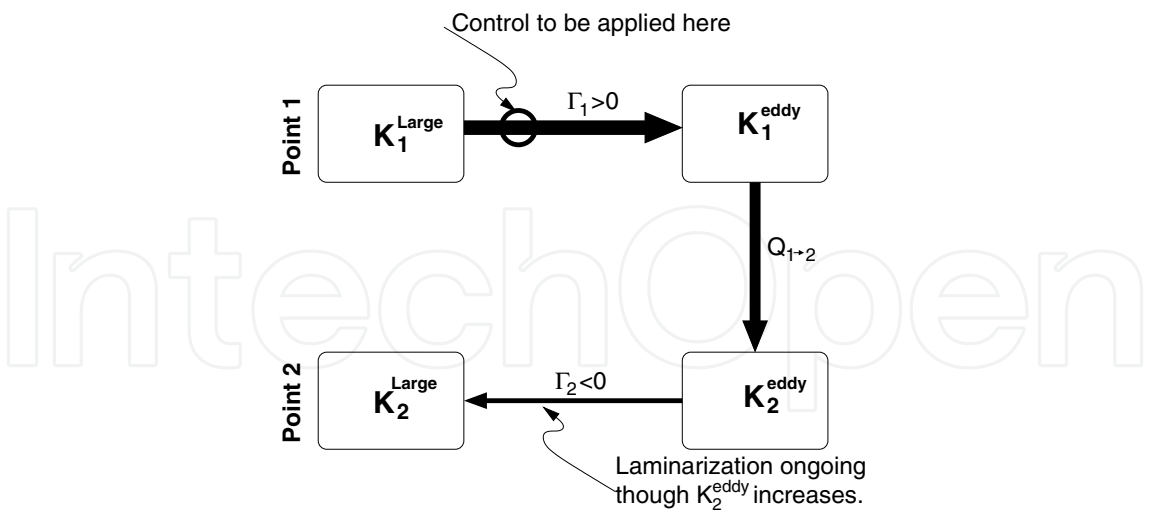

Fig. 12. Schematic of the energetics in a two-point system. We use K, Γ, and Q to signify energy, transfer, and transport, respectively. In this case, both K_1^{eddy} and K_2^{eddy} grow, but their mechanisms are different. The former is due to an instability, while the latter comes from the positive offset $|Q_{1\to2}| - |\Gamma_2|$, although the transfer $\Gamma_2 < 0$ is in the inverse direction. To take advantage of the inverse transfer or laminarization, the control should be placed at point 1 only. (Adapted from Liang and Wang, 2004.)

is transported from the former. The transfer Γ_2 at point 2 is toward the large-scale window, i.e., a laminarization is taking place there, but since $Q_{1\to2} - |\Gamma_2| > 0$, K_2^{eddy} still grows. Of course, control of the perturbation energy growth at both points 1 and 2 does help to suppress the onset of turbulence, but it is not optimal in terms of energy saving. Suppression of K_2^{eddy} also suppresses the intrinsic trend of laminarization at point 2, and therefore reduces the control performance. An optimal control strategy should take advantage of this trend, implying that the control should be applied at point 1 only. Besides, the optimal objective functional should be chosen to be Γ_1, rather than $K_1^{eddy} + K_2^{eddy}$. With this, we have proposed a strategy to harness vortex shedding behind a circular cylinder, and obtained satisfactory, albeit preliminary, results (e.g., Liang, 2007). We shall explore more about this in future studies.

12. Acknowledgments

13. Appendix: Detailed balance relation

It has been a common practice to check if the interaction analysis satisfies a Jacobian identity-like *detailed balance relation* (e.g., Lesieur 1990; Iima and Toh 1995). We show this is true with our formulation with the incompressibility assumption. For a scalar field T, and flow $\mathbf{v}$, the transfer at n on window ϖ, Γ_n^ϖ, is given by (21). The basic transfer function of Γ_n^ϖ is, by our definition in section 7,

$$
\begin{aligned}
&Tr\,(n_1, \varpi_1 \mid n_2, \varpi_2; n_3, \varpi_3) = \\
&\frac{1}{2}\left[-\widehat{T}_{n_1}^{\sim\varpi_1}\nabla\cdot\left(\widehat{\mathbf{v}}_{n_2}^{\sim\varpi_2}\widehat{T}_{n_3}^{\sim\varpi_3}\right) + \frac{1}{2}\nabla\cdot\left(\widehat{T}_{n_1}^{\sim\varpi_1}\widehat{\mathbf{v}}_{n_2}^{\sim\varpi_2}\widehat{T}_{n_3}^{\sim\varpi_3}\right)\right]\widehat{(\phi_{n_2}^{j_2}\phi_{n_3}^{j_3})}_{n_1}^{\sim\varpi_1} \\
&+\frac{1}{2}\left[-\widehat{T}_{n_1}^{\sim\varpi_1}\nabla\cdot\left(\widehat{\mathbf{v}}_{n_3}^{\sim\varpi_3}\widehat{T}_{n_2}^{\sim\varpi_2}\right) + \frac{1}{2}\nabla\cdot\left(\widehat{T}_{n_1}^{\sim\varpi_1}\widehat{\mathbf{v}}_{n_3}^{\sim\varpi_3}\widehat{T}_{n_2}^{\sim\varpi_2}\right)\right]\widehat{(\phi_{n_2}^{j_2}\phi_{n_3}^{j_3})}_{n_1}^{\sim\varpi_1},
\end{aligned}
\tag{38}
$$

for windows ϖ_1, ϖ_2, ϖ_3, and locations n_1, n_2, n_3 in the time sampling space. When the flow is incompressible (hence $\nabla\cdot\widehat{\mathbf{v}}_n^{\sim\varpi} = 0$ for any ϖ and n), it is straightforward check that

$$
\begin{aligned}
Tr\,(n_1, \varpi_1 \mid n_2, \varpi_2; n_3, \varpi_3) &+ Tr\,(n_2, \varpi_2 \mid n_3, \varpi_3; n_1, \varpi_1) \\
&+ Tr\,(n_3, \varpi_3 \mid n_1, \varpi_1; n_2, \varpi_2) = 0.
\end{aligned}
\tag{39}
$$

This is the detailed balance relation.

14. References

[1] Briggs, R.J. (1964). Criteria for identifying amplifying waves and absolute instabilities. *Electro-Stream Interaction with Plasamas.* The MIT Press, 8-46.

[2] Carnevale, G.F. & Frederiksen, J.S. (1987). Nonlinear stability and statistical mechanics of flow over topography. *J. Fluid. Mech.*, Vol. 175:157-181.

[3] Drazin, P.G. & Reid, W. H. (1982). *Hydrodynamic stability*, Cambridge University Press.

[4] Germano, M., Piomelli, U., Moin, P., & Cabot, W.H. (1991). A dynamic subgrid-scale eddy viscosity model. *Phys. Fluids A*, Vol. 3:1760-1765.

[5] Gill, A.E. (1982). *Atmosphere-Ocean Dynamics*, Academic Press.

[6] Godreche, C. & Manneville, P. (1998). *Hydrodynamics and Nonlinear Instabilities,* Cambridge University Press.

[7] Haley, P.J., Lermusiaux, P.F.J., Robinson, A.R., Leslie, W.G., Logoutov, O., Cossarini, G., Liang, X.S., Moreno, P., Ramp, S.R., Doyle, J.D., Bellingham, J., Chavez, F., & Johnston, S. (2009). Forecasting and reanalysis in the Monterey Bay/California Current region for the Autonomous Ocean Sampling Network-II experiment, *Deep-Sea Res.*, Part II, Vol. 56 (3-5):127-148.

[8] Huang, N. E., Shen, Z. & Long, S.R. (1999). A new view of nonlinear water waves: The Hilbert spectrum, *Annu. Rev. Fluid Mech.*, Vol. 31:417-457.

[9] Huerre, P. & Monkewitz, P. A. (1990). Local and global instabilities in spatially developing flows, *Annu. Rev. Fluid Mech.*, Vol. 22:473-537.

[10] Iima, M. & Toh, S. (1995). Wavelet analysis of the energy transfer caused by convective terms: Application to the Burgers shock, *Phys. Rev. E*, Vol. 52(6):6189-6201.

[11] Lesieur, M. (1990). *Turbulence in Fluids: Stochastic and Numerical Modeling,* 2nd ed., Klumer Academic Publishers.

[12] Liang, X. San (2007). Perfect transfer and mean-eddy interaction in incompressible fluid flows. arXiv:physics/0702002. http://arxiv.org/abs/physics/0702002.

[13] Liang, X. San & Anderson, Donald G. M. (2007). Multiscale window transform, *SIAM J. Multiscale. Model. Simu.*, Vol 6(2):437-467.

[14] Liang, X. San & Robinson, Allan R. (2005). Localized multiscale energy and vorticity analysis: I. Fundamentals, *Dyn. Atmos. Oceans*, Vol 38:195-230.

[15] Liang, X. San & Robinson, Allan R. (2007). Localized multiscale energy and vorticity analysis: II. Finite-amplitude instability theory and validation, *Dyn. Atmos. Oceans*, Vol 44:51-76.

[16] Liang, X. San & Wang, Meng (2004). A study of turbulent wake dynamics using a novel localized stability analysis. Center for Turbulence Research, *Proceedings of the Summer Program 2004*, 211-222.

[17] Lifschitz, A. (1994). On the instability of certain motions of an ideal incompressible fluid, *Advances in Applied Mathematics*, Vol 15:404-436.

[18] Lilly, D.K. (1992): A proposed modification of the Germano subgrid scale closure method, *Phys. Fluids A*, Vol 4:633-635.

[19] Lin, C.C. (1966): *The theory of hydrodynamic stability*, Cambridge U Press.

[20] Mittal, R. & Moin, P. (1997). Suitability of upwind-biased finite difference schemes for large-eddy simulation of turbulence flows, *AIAA J.*, Vol. 35:1415-1417.

[21] Oertel, H., Jr. (1990). Wakes behind blunt bodies, *Annu. Rev. Fluid Mech.*, Vol 22:539-558.

[22] Pierrehumbert, R. T. & Swanson, K. L. (1995). Baroclinic Instability, *Ann. Rev. Fluid Mech.*, Vol. 27:419-467.

[23] Pope, S. (2003). *Turbulent Flows*, Cambridge University Press.

[24] Schmid, P.J. & Henningson, D. S. (2001). *Stability and transition in shear flows*, Springer, New York.

[25] Strang, G. & Nguyen, T. (1997). *Wavelets and Filter Banks,* Wellesley-Cambridge Press.

[26] Pastoor, M., Henning, L., Noack, B.R., King, R., & Tadmor, G., (2008). Feedback shear layer control for bluff body drag reduction, *J. Fluid Mech.*, Vol. 608:161-196.

[27] Williamson, C. H. K. (1996). Vortex dynamics in the cylinder wake, *Ann. Rev. Fluid Mech.*, Vol. 28:477-526.
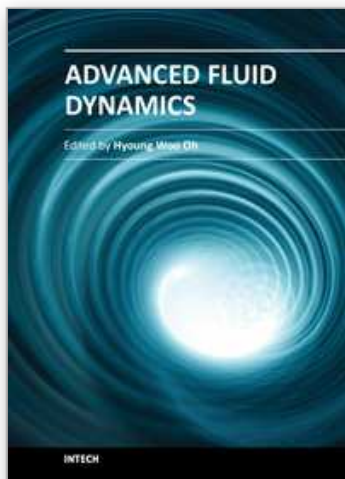
Advanced Fluid Dynamics

Edited by Prof. Hyoung Woo Oh

This book provides a broad range of topics on fluid dynamics for advanced scientists and professional researchers. The text helps readers develop their own skills to analyze fluid dynamics phenomena encountered in professional engineering by reviewing diverse informative chapters herein.

How to reference

In order to correctly reference this scholarly work, feel free to copy and paste the following:

X. San Liang (2012). Multiscale Window Interaction and Localized Nonlinear Hydrodynamic Stability Analysis, Advanced Fluid Dynamics, Prof. Hyoung Woo Oh (Ed.), ISBN: 978-953-51-0270-0, InTech, Available from: http://www.intechopen.com/books/advanced-fluid-dynamics/multiscale-window-interaction-and-localized-nonlinear-hydrodynamic-instability-analysis